RESEARCH ARTICLE

Exploring the Coordination, Anti-oxidant, and Bacterial Behavior of a New Azo Ligand Derived from 4,5-Dimethylimidazole with Copper and Zinc Divalent Ions

Husham M. Mubarak
Israa N. Witwit
Hussein A. Ali Salman
Mohauman M. Al Rufaie

Authors' address:
Chemistry Department, College of Sciences, University of Kufa, Najaf, Iraq

Correspondence:
Husham M. Mubarak
Chemistry Department, College of Sciences, University of Kufa, Najaf, Iraq
Tel.: +9647810106496
e-mail: HushamMMubark@yahoo.com

Article info:
Received: 15 May 2024
Accepted: 21 November 2024

ABSTRACT
New azo ligand synthesized from 4, 5-dimethylimidazole, focusing on its coordination properties with copper and zinc divalent ions. The experimental findings confirmed the formation of octahedral geometrical complexes, where the coordination occurs through one nitrogen atom of azo and an N3 atom of imidazole. Evidence from spectroscopic techniques (^{13}-CNMR, Mass, FT-IR, and UV-Vis), conductivity measurements, and magnetic susceptibility supported the structural integrity of the complexes. Biological evaluation showed that the ligand and its complexes possess notable antibacterial properties, particularly the zinc complex, which exhibited stronger inhibitory effects against both *Staphylococcus and E. coli* bacteria. Antioxidant tests using the DPPH assay indicated that the ligand effectively scavenges free radicals, achieving 70% inhibition at 25 ppm, making it a promising candidate when compared to ascorbic acid. The results underscore the potential of this ligand and its complexes for applications in medicinal chemistry, especially in the development of antimicrobial and antioxidant agents.

Keywords: Azo ligand; 4,5-Dimethylimidazole; Antibacterial activity; Antioxidant activity; DPPH; Octahedral geometry; Spectroscopic analysis

Introduction

Imidazole-azo ligands represent a distinctive category of chelating agents that have attracted considerable interest in coordination chemistry and materials science (Jawad & Al-Adilee, 2022; Mgheer et al., 2022). Their uniqueness lies in the integration of imidazole and azo groups that synergistically enhance their ability to form robust interactions with diverse metal ions. The imidazole ring, renowned for its electron-donating capability, significantly strengthens the coordination potential of the ligand, while the azo group (–N=N–) contributes additional stability and structural versatility in complex formation (Puratchikody & Doble, 2007; Ward et al., 2022).

The synthesis of imidazole-azo ligands typically involves reacting imidazole derivatives with azo coupling agents (Mahmoud et al., 2015; Mezgebe & Mulugeta, 2022) resulting in a range of ligands with tunable properties. These ligands exhibit excellent solubility in organic solvents and can be tailored to possess specific optical and electronic characteristics, making them suitable for applications in catalysis, sensors, and advanced material development. Moreover, imidazole-azo ligands have shown promising biological activities (Concilio et al., 2015), including antimicrobial (Romero et al., 2014; Atiya et al., 2023) and anticancer effects (Sen et al., 2018; Sharma et al., 2021; Ribeiro et al., 2023;). Their strong affinity for forming stable complexes with transition metals further enhances their potential for use in drug delivery systems and therapeutic applications (Chhetri et al., 2021a; Chhetri et al., 2021b).

This research aims to synthesize a new azo ligand, previously unreported, derived from 4,5-dimethylimidazole, and to investigate its coordination behavior with two biologically significant metal ions, Cu^{2+} and Zn^{2+}. Following this, an applied study will be conducted to evaluate the antibacterial activity of the new ligand and its prepared complexes against both Gram-positive and Gram-negative bacteria. Additionally, their antioxidant properties will be assessed in comparison to ascorbic acid as a standard reference.

Materials and Methods

Chemicals and Instruments

All solid and liquid chemicals were obtained from B.H.D., Merck, Fluka, and AK Scientific, and were of high purity. Magnetic susceptibility measurements for the solid, purified complexes were conducted using the Balance Magnetic Susceptibility Design (M. S. B Auto). Mass spectrometry analysis was carried out with a SCIEX 3200 Mass Analyzer, while FT-IR spectra were acquired using a Shimadzu 8400.

Electronic spectra were recorded with a Shimadzu UV-1650 Spectrophotometer, and molar conductivity was assessed using a 720-WTW.

Perpetration of (DMIA)

The ligand was prepared by mixing 10 mmol (1.38 g) of 4-nitroaniline with 3 ml of hydrochloric acid in 25 ml of distilled water, maintaining the temperature between 0-5°C. A sodium nitrite solution, prepared by dissolving 0.7 g of sodium nitrite in 10 ml of distilled water, was added dropwise with continuous stirring. The resulting diazonium salt solution was left for 30 minutes to stabilize. The stabilized solution was then gradually added to the alcoholic solution of 4,5-dimethylimidazole, prepared by dissolving 10 mmol (0.96 g) of the compound in 25 ml of ethanol. After the addition was complete, an orange precipitate formed, which was filtered, washed, dried, and recrystallized from hot ethanol, as shown in Scheme 1.

Preparation of solid complexes

The solid complexes were prepared in a molar ratio of (2:1)

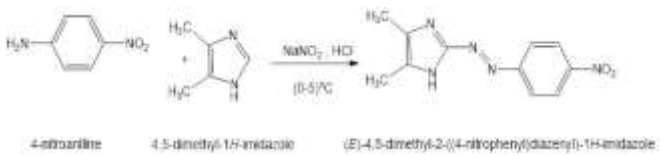

Scheme 1. *The reaction equation for the synthesis of the new ligand (DMIA).*

(Metal: Ligand) by mixing (2 mmole, 0.238 g) of the ligand (DMIA) with (1 mmole, 0.136 g) of $ZnCl_2$ salt and (1 mmole, 0.170 g) of $CuCl_2 \cdot 2H_2O$, each separately in (30) ml of ethanol, until the precipitates of the complexes appeared. The complexes were then filtered, dried, and recrystallized from hot ethanol. The general preparation equation for the solid complexes is illustrated in Scheme 2.

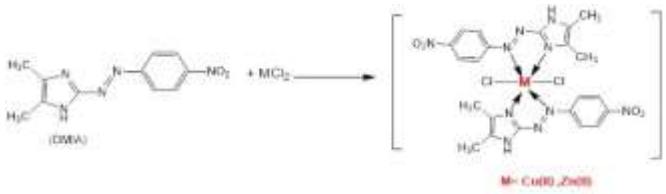

Scheme 2. *The reaction equation for the synthesis of the complexes of Cu(II), and Zn(II) with (DMIA).*

Measurement of Antibacterial Efficacy

The agar well diffusion method was used to prepare the growth medium for the pathogenic bacteria used. The nutrient agar was prepared with the bacterial suspension using a prepared cotton swab. Wells were created with a cork borer, with each well having a diameter of 6 mm in the growth medium. Two wells were kept as controls: one containing distilled water and the other containing DMSO solvent. The bacterial plates were incubated for 24 hours at a temperature of 37°C. The efficacy of the complex was then determined by measuring the diameter of the inhibition zone (Inhibition Zone) in millimeters around each well for two types of pathogenic bacteria (*Staphylococcus spp.* and *E. coli*).

Measurement of Anti-oxidant activity

The antioxidant ability of the newly synthesized ligand was evaluated using the stable free radical (DPPH) assay and compared with ascorbic acid as a reference standard. Solutions of the ligand were prepared at concentrations of 5, 10, 15, 20, and 25 ppm in methanol. A 0.3 mL aliquot of each ligand solution was mixed with 2.7 mL of ethanolic DPPH solution (0.004% w/v). Each mixture was prepared individually and incubated in the dark at room temperature. After 30 minutes of reaction time, the absorbance was measured at 517 nm to assess the ligands.

Results and Discussion

Mass fragmentation of (DMIA) ligand

Mass spectrometry is a powerful analytical technique that confirms the molecular formula of the compound and provides insights into its fragmentation pathways. The mass spectrum of DMIA revealed a molecular ion peak at *m/z* = 245, corroborating the molecular structure of this new compound. The base peak, with 100% relative abundance, appeared at *m/z* = 217.2, corresponding to the molecular ion $[C_9H_7N_5O_2]^+$. Two primary fragmentation pathways were proposed: one involving the partial loss of an N_2 molecule, and the other resulting from the dissociation of the ligand via cleavage of two methyl groups. As shown in Figure 1 and Scheme 3.

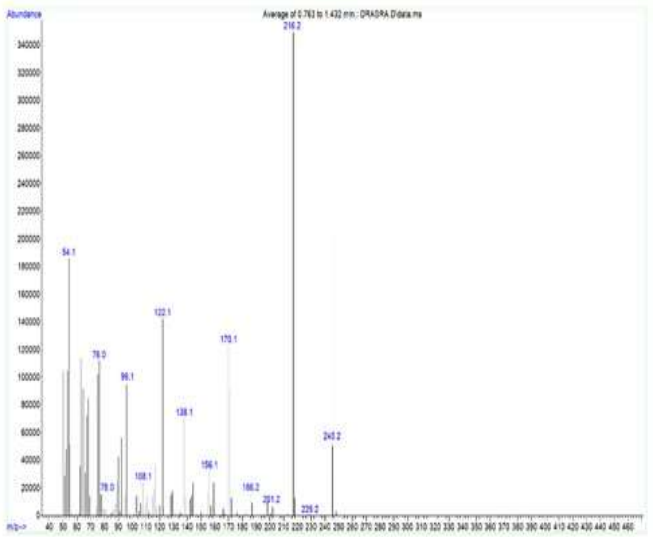

Figure 1. *Mass Spectrum of (DMIA) ligand.*

http://www.jbb.uni-plovdiv.bg DOI: 10.69085/jbb20242133

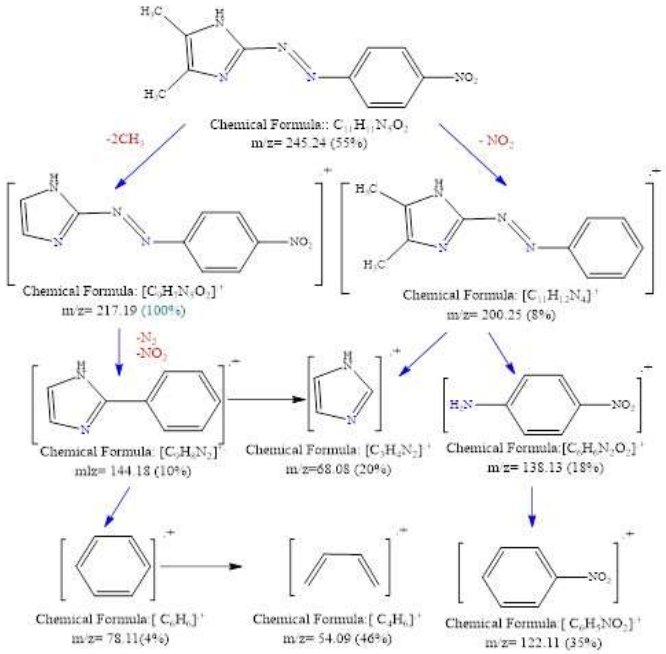

Scheme 3. *Mass Fragmentation paths of (DMIA) ligand.*

^{13}C-NMR of (DMIA) ligand

The ^{13}C-NMR spectrum of the DMIA ligand recorded in DMSO-d^6 exhibited signals in the range of 31.5 – 40.75 ppm, corresponding to residual solvent peaks. A distinct peak at 13.6 ppm was attributed to the methyl groups substituted on the heterocyclic imidazole ring (-CH_3). The signals observed at 139.6, 148.1, and 146.6 ppm were assigned to the carbon atoms C2, C4, and C5 of the imidazole ring, respectively. Additionally, signals in the 122.8–135.4 ppm range corresponded to aromatic carbons of the benzene ring. These chemical shifts provide valuable insights into the number, type, and positions of carbon atoms within the molecular framework, as illustrated in Figure 2.

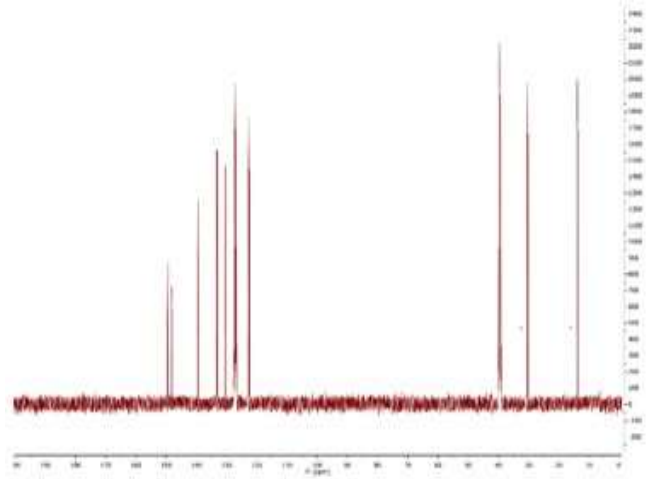

Figure 2. *^{13} C-NMR spectrum of (DMIA) Ligand.*

FT-IR Spectrum of (DMIA) and its complexes

Infrared (IR) spectroscopy is a reliable method for identifying the active functional groups in the compounds under investigation. The IR spectrum of the newly synthesized DMIA ligand displayed characteristic frequencies corresponding to the imidazole ring (including the stretching vibrations of *v*(C=N), *v*(C–N), and *v* (N=N) at 1534 cm^{-1}, 902 cm^{-1}, and 1417 cm^{-1}, respectively. In the spectra of the metal complexes, significant shifts and intensity variations were observed, indicating the involvement of both the imidazole ring and the bridged azo group in coordination (Witwit et al., 2019; Witwit et al., 2020; Fnfoon & Al-Adilee, 2023). These vibrations appeared at 1517 cm^{-1}, 912 cm^{-1}, and 1411 cm^{-1} for the Cu (II) complex, and at 1517 cm^{-1}, 918 cm^{-1}, and 1418 cm^{-1} for the Zn (II) complex. Additionally, new absorption bands corresponding to the metal-nitrogen *v* (M–N)) bonds were detected at 455 cm^{-1} for the Cu (II) complex and 436 cm^{-1} for the Zn (II) complex, as illustrated in Figures 3-5.

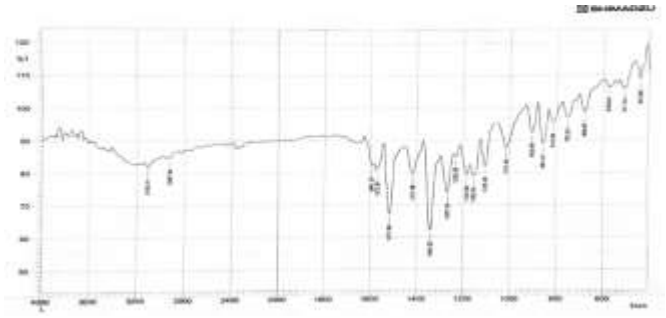

Figure 3. *FT-IR spectrum of (DMIA) Ligand.*

Figure 4. *FT-IR spectrum of Cu(II) complex.*

Figure 5. *FT-IR spectrum of Zn(II) complex.*

Table 1. *Elemental Analysis, Molar Conductivity of (DMIA), and the complexes*

Compound (Molecular Formula)	Molar Conductivity S.Cm^2.mole-		M.P.	Colour	Elemental Analysis Calculated (Found)		
	Ethanol	(DMSO)			C	H	N
(DMIA) $C_{11}H_{11}N_5O_2$	------	-----	174-176	Orange	53.87 (53.91)	4.52 (4.50)	28.56 (28.60)
$[Cu(DMIA)_2Cl_2]$ $C_{22}H_{22}Cl_2CuN_{10}O_4$	12.3	15.0	187-189	Brown	42.28 (42.31)	3.55 (3.52)	22.41 (22.43)
$[Zn(DMIA)_2Cl_2]$ $C_{22}H_{22}Cl_2ZnN_{10}O_4$	10.6	12.5	194-196	Red	42.16 (42.18)	3.54 (3.57)	22.35 (22.36)

Electronic Spectra of the ligand, and complexes

Ultraviolet-visible spectroscopy (UV-Vis) is a successful method for studying the types of electronic transitions in the compounds under investigation. The UV-Vis spectrum of the primary ligand (DMIA) showed two bands at wavelengths of 204 nm and 227 nm, corresponding to (π-π*) transitions, and two bands at wavelengths of 364 nm and 372 nm, corresponding to (n-π*) transitions and intramolecular charge transfer (ICT) transitions of the ligand. These bands experienced a noticeable shift toward longer wavelengths in the spectra of the complexes as a result of the coordination process (Figure 6-8).

Elemental Analysis, molar conductivity, and magnetic properties:

The elemental analysis (C.H and N) of the ligand and the prepared complexes showed a high degree of agreement between the experimental values and the theoretically calculated values, confirming the molecular formulas of the studied compounds. Conductivity measurements in ethanol and dimethyl sulfoxide solvents indicated that the prepared complexes do not possess ionic properties, and the chloride ions are incorporated within the coordination sphere. This is further supported by the absence of silver chloride precipitation upon adding silver nitrate drops to the complex solution, as well as the significant difference in melting points between the prepared complex and the parent ligand, along with the distinct colours of their precipitates, as shown in Table 1.

Magnetic susceptibility measurements, conducted using the Gouy method and employing Pascal's diamagnetic correction tables, indicated that the copper complex possesses a value of 1.97 Bohr magnetons. This value confirms the electronic configuration [Ar] $3d^9$ of the copper (II) ion (Sun et al., 2017; Witwit et al., 2023) and its distorted octahedral geometry. In contrast, the zero value of magnetic susceptibility observed for the zinc complex suggests that it exhibits diamagnetic characteristics with electronic configuration [Ar] $3d^{10}$.

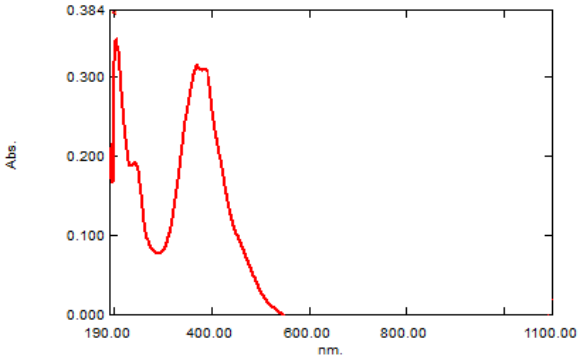

Figure 6. *UV-Vis spectrum of (DMIA) Ligand.*

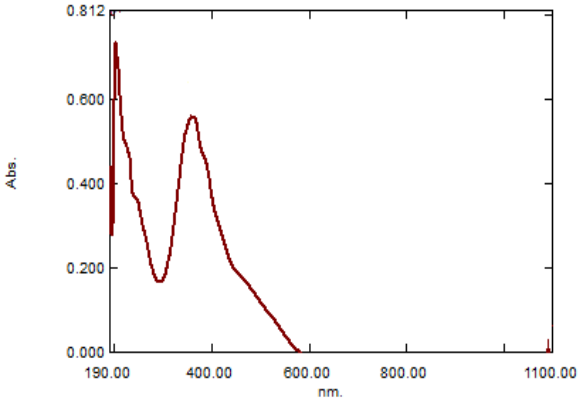

Figure 7. *UV-Vis spectrum of Cu(II) complex.*

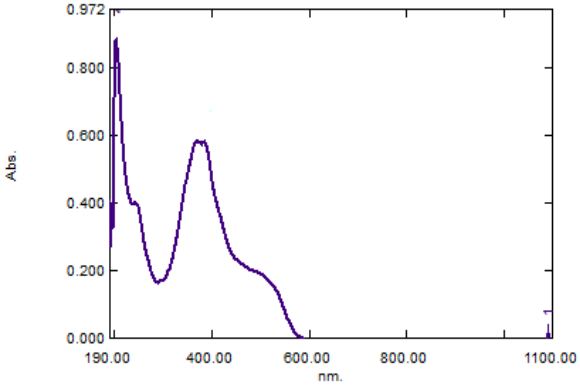

Figure 8. *UV-Vis spectrum of Zn(II) complex.*

http://www.jbb.uni-plovdiv.bg DOI: 10.69085/jbb20242133

According to the results obtained, an octahedral configuration has been suggested for the two synthesized complexes. In this structure, the ligand bonds to the divalent copper and zinc ions via the nitrogen atom at position (3) of the imidazole heterocyclic ring and one of the nitrogen atoms from the azo group, forming a stable five-membered ring around the central ion. The remaining coordination sites are occupied by two chloride ions, as depicted in the Figure 9.

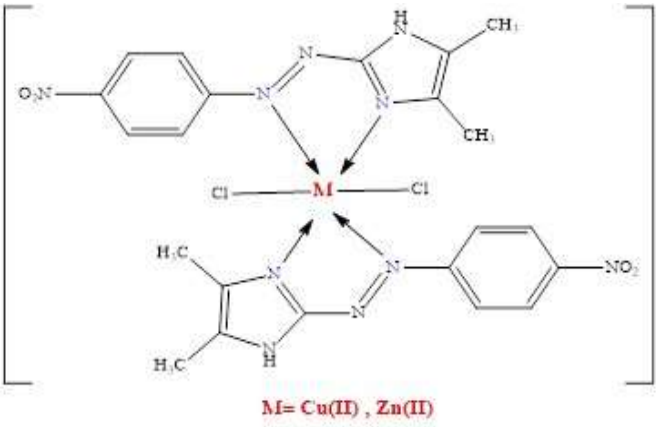

Figure 9. *Suggested structure of the prepared complexes.*

Antioxidant activity of (DMIA) ligand

This method provides a reliable approach to evaluating the antioxidant activity of free ligand by measuring their ability to scavenge DPPH radicals (de Sá Junior et al., 2017). The free radical scavenging activity was determined using a stable radical DPPH (Diphenylpicrylhydrazyl) that accepts an electron or hydrogen atom to become a stable diamagnetic molecule. When the DPPH radical reacts with an antioxidant compound capable of donating a hydrogen atom, it changes colour from deep violet to pale yellow. The degree of discoloration indicates the scavenging potential of the antioxidant compound. This process is monitored by measuring the decrease in absorbance at a specific wavelength using a spectrophotometer. The higher the reduction in DPPH absorbance, the more effective the compound is in scavenging free radicals (Figure 10).

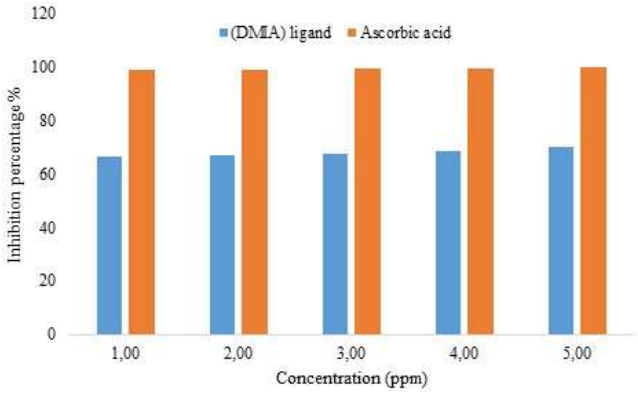

Figure 10. *Antioxidant activity of (DMIA) ligand against Ascorbic acid.*

The reduction in absorbance at (517) nm directly correlates with the antioxidant potential of the compounds under study, allowing for quantitative comparison across different concentrations and with Ascorbic acid as a reference standard from a period of concentration (5-25) ppm. The higher percentage of Inhibition for the free ligand at (25) ppm, as shown in Table 2.

Table 2. *Inhibition percentage of (DMIA) ligand against Ascorbic acid as Anti-oxidants.*

Conc.	(DMIA) ligand		Ascorbic acid	
(ppm)	Absorbance	Inhibition%	Absorbance	Inhibition%
5	0.335	66.5	0.335	66.5
10	0.328	67.2	0.328	67.2
15	0.324	67.6	0.324	67.6
20	0.316	68.8	0.316	68.8
25	0.300	70.0	0.300	70.0

Anti-bacterial activity of (DMIA) ligand, and the complexes

The measurements of the antibacterial activity of bacteria are crucial applications that serve as the foundation for evaluating and testing prepared materials as pharmaceutical agents (Abd Al-Sadda et al., 2019; Kadhium et al., 2019). The mechanisms through which ligands and metal complexes can inhibit bacteria involve multiple interactions affecting the cell wall, proteins, and nucleic acids, as well as the generation of free radicals.

Two common pathogenic bacterial strains were selected: *Staphylococcus aureus*, classified as Gram-positive, and *Escherichia coli*, classified as Gram-negative. As shown in Table 3 and Figures 11 and 12. At 150 mg/mL *S. aureus* exhibited greater resistance to inhibition compared to *E. coli* when exposed to the free ligand and its metal complexes. This difference can be attributed to the thick cell wall characteristic of Gram-positive bacteria, along with their enhanced ability to disseminate resistance genes through horizontal gene transfer.

Table 3. *Inhibition percentage of (DMIA) ligand against Ascorbic acid as Anti-oxidants.*

Compound	*E. coli* R= 4, ME±SE	*S. aureus* R= 4, ME±SE
(DMIA)	12.5± 0.28	9.63± 0.24
[Cu(DMIA)$_2$Cl$_2$]	16.75± 0.24	13.87± 0.10
[Zn(DMIA)$_2$Cl$_2$]	22.65± 0.24 ±	17.87± 0.27

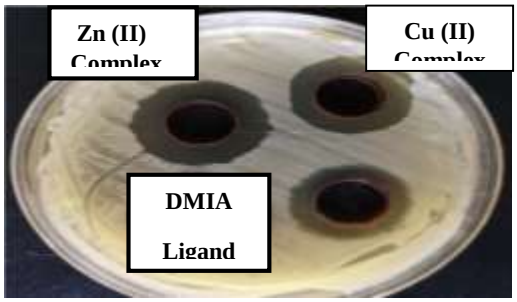

Figure 11. *Inhibition area of (DMIA) and the complexes against Staphylococcus aureus.*

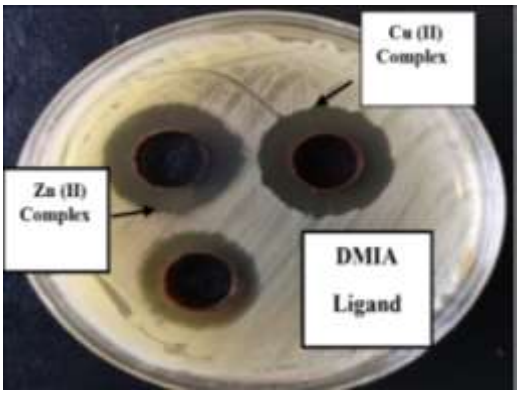

Figure 12. *Inhibition area of (DMIA) and the complexes against Escherichia coli.*

Conclusions

This study successfully synthesized a new azo ligand from 4,5-dimethylimidazole, demonstrating strong coordination with copper and zinc ions. The ligand exhibited significant antibacterial activity against various strains and effective antioxidant properties in scavenging free radicals. These findings highlight the potential of imidazole-azo ligands for applications in catalysis and medicinal chemistry, positioning the synthesized ligand and its complexes as promising candidates for further research in pharmaceutical applications.

References

Al-Sadda H, al Hussainawy M, Kyhoiesh H. 2019. Spectral Characterization and Biological Activity of 2-[2¯-(1-Amino-1,5-Dinitrophenyl)azo]-Imidazole. J. Glob. Pharma Technol., 11(7): 165-174.

Atiya RN, Razzaq ZL, Yahya WI, Neamah HM. 2023. Synthesis, Characterization and Studying Biological Activity of Heterocyclic Compounds. Int. J. Drug Deliv. Technol., 13(1): 205-211. doi: 10.25258/ijddt.13.1.31

Chhetri A, Chettri S, Rai P, Mishra DK, Sinha B, Brahman D. 2021a. Synthesis, characterization and computational study on potential inhibitory action of novel azo imidazole derivatives against COVID-19 main protease (Mpro: 6LU7). J Mol Struct., 1225: 129230. doi:10.1016/j.molstruc.2020.129230

Chhetri A, Chettri S, Rai P, Sinha B, Brahman D. 2021b. Exploration of inhibitory action of Azo imidazole derivatives against COVID-19 main protease (Mpro): A computational study. J Mol Struct., 1224: 129178. doi:10.1016/j.molstruc.2020.129178

Concilio, S., Iannelli, P., Sessa, L., Olivieri, R., Porta, A., De Santis, F., Pantani, R. and Piotto, S. 2015. Biodegradable antimicrobial films based on poly(lactic acid) matrices and active azo compounds. J. Appl. Polym. Sci., 132: 42357. doi: 10.1002/app.42357

de Sá Junior PL, Câmara DAD, Porcacchia AS, et al. The Roles of ROS in Cancer Heterogeneity and Therapy. Oxid Med Cell Longev, 2017: 2467940. doi:10.1155/2017/2467940

Fnfoon DY, Al-Adilee KJ. 2023. Synthesis and spectral characterization of some metal complexes with new heterocyclic azo imidazole dye ligand and study biological activity as anticancer, J. Mol. Struct., 1271: 134089.

Jawad SH, Al-Adilee KJ. 2022. Synthesis and characterization of a new 1-methyl imidazole derived ligand with its ionic complexes Pd(II) and Pt(IV) and study of biological activity as anticancer and antioxidant. Results in Chemistry, 4(1) :1-18.

Kadhium A, Mahdi S, Alrammahi F. 2019. Preparation and Characterization of new Azo/Azo-Chalcone Ligands and their mixed ligands transition metal complexes with A study of Palladium Complex Anticancer Activity. Res J Pharm Technol., 12: 5947-5955. doi: 10.5958/0974-360X.2019.01032.1.

Mahmoud WA, Ali AAM, Kareem TA. 2015 Preparation and Spectral Characterization of New Azo Imidazole Ligand 2-[(2`-Cyano Phenyl) Azo]-4,5-Diphenyl Imidazole and its Complexes with Co(II), Ni(II), Cu(II), Zn(II), Cd(II) and Hg (II) Ions. Baghdad Sci. J.; 12(1): 96-109.

Mezgebe K, Mulugeta E. 2022. Synthesis and pharmacological activities of azo dye derivatives incorporating heterocyclic scaffolds: a review. RSC Adv., 12(40): 25932-25946. doi: 10.1039/d2ra04934a

Mgheer TH, Abdulmahdi BS, Mohammed LA. 2022. Bio-Chemical study and preparation of some new mixed ligand complexes with novel(azo) ligand derived from5-methyl imidazole and 1,10-phenanthroline compounds. Journal of Pharmaceutical Negative Results, 13(7): 7135-7146. doi: 10.47750/pnr.2022.13.S07.861

Puratchikody A, Doble M. 2007. Antinociceptive and antiinflammatory activities and QSAR studies on 2-substituted-4,5-diphenyl-1H-imidazoles. Bioorg Med Chem., 15(2): 1083-1090. doi:10.1016/j.bmc.2006.10.025

Ribeiro AI, Vieira B, Dantas D, Silva B, Pinto E, Cerqueira F, Silva R, Remião F, Padrão J, Dias AM, Zille A. 2023. Synergistic Antimicrobial Activity of Silver Nanoparticles with an Emergent Class of Azoimidazoles. *Pharmaceutics*, 15(3): 926. doi:10.3390/pharmaceutics15030926

Romero DH, Heredia VET, García-Barradas O, Márquez López ME, Sánchez Pavón E. 2014. Synthesis of Imidazole Derivatives and Their Biological Activities. J. Chem. Biol., 2(2): 45-83.

Sen C., Patra C, Mondol S, Datta A, Mallick D, Mondal TK, Askun T, Celikboyun P, Cantürk Z, Sinha C. 2018. Platinum (II)-azoimidazole drugs against TB and cancer: structural studies, cytotoxicity and anti-mycobacterial activity. Polyhedron, 158: 1-30. doi: 10.1016/j.poly.2018.05.062

Sharma P, LaRosa C, Antwi J, Govindarajan R, Werbovetz KA. 2021. Imidazoles as Potential Anticancer Agents: An Update on Recent Studies. Molecules, 26(14): 4213. doi:10.3390/molecules26144213

Sun Y-J, Diao Y-F, Wang H-G, Chen G, Zhang M, Guo M. 2017. Synthesis, structure and magnetic properties of spinel ferrite (Ni, Cu, Co) Fe_2O_4 from low nickel matte. Ceramics International 43 (18): 16474-16481.

Ward HA, Musa TM, Nasif ZN. 2022. Synthesis and Characterization of some Transition Metals Complexes with new Ligand Azo Imidazole Derivative. Al-Mustansiriyah J. Sci., 33(2): 31-38. doi:10.23851/mjs.v33i2.1121

Witwit IN, Mubark HM, Al-Labban HMY, Aljanaby AAJ 2019. Synthesis and characterization of new imidazole azo ligand with some of transition metal ions, and their biological effect on two pathogenic bacteria of burn patients, Int. J. Pharm. Sci. Res., 10(3) :1847-1856.

Witwit IN, Mubarka HM, Motaweqb ZY, Al Rufaie MM. 2023. Synthesis, Bacterial Inhibition, and coordination behavior study of new Azoimidazole ligand with some of first series transition ions. Acta Chemica Lasi, 31(2): 129-146.

Witwit IN, Mubarka HM, Ali AAM. 2020. Synthesis and studying the coordination behavior of a new heterocyclic imidazole azo ligand with some of the first series transition and (IIB) ions. AIP Conference Proceedings, 2290: 030025.